AD-A141 918 IMPROVED MULTI-TARGET TIME DELAY ESTIMATION: MATCHED 1/1
FILTER APPROACH(U) NAVAL UNDERWATER SYSTEMS CENTER NEW
LONDON CT NEW LONDON LAB W K FISCHER 29 MAY 84
UNCLASSIFIED NUSC-TR-7149 F/G 12/1 NL

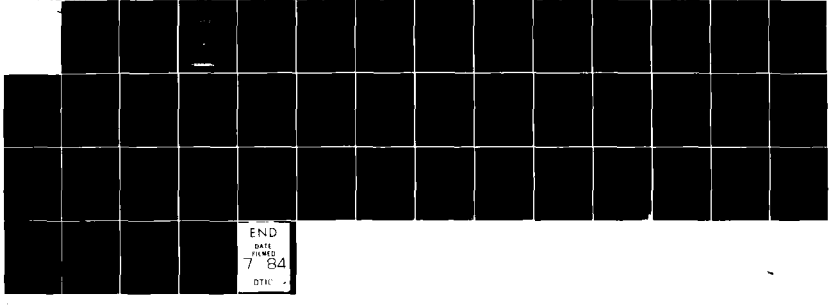

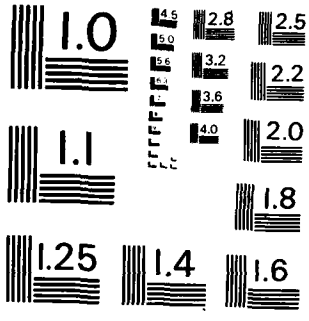

(12)

NUSC Technical Report 7149
29 May 1984

Improved Multi-Target Time Delay Estimation: Matched Filter Approach

Wolfgang K. Fischer
Submarine Sonar Department

Naval Underwater Systems Center
Newport, Rhode Island / New London, Connecticut

PREFACE

This research was conducted jointly for NRL Project No. A12216, Subproject No. SD022, "ASW System Performance Analysis," Principal Investigator, P. Bean (Code 5270), engineering activity, Naval Sea Systems Command (PMS-407) and for NRL Project No. B47000, Subproject No. S1347-AB, "Acoustic Transducer Engineering," Principal Investigator, L. Ng (Code 5218), engineering activity Naval Sea Systems Command (PMS-402).

The Technical Reviewer for this report was L. Ng (Code 5218).

REVIEWED AND APPROVED 29 May 1985

F. J. Gaghan

Head, Underwater Sound Division

REPORT DOCUMENTATION PAGE	READ INSTRUCTIONS BEFORE COMPLETING FORM
1. REPORT NUMBER: TR 7149	2. GOVT ACCESSION NO.: AD-A141918
3. RECIPIENT'S CATALOG NUMBER:	
4. TITLE (and Subtitle): IMPROVED MULTI-TARGET TIME DELAY ESTIMATION: MATCHED FILTER APPROACH	5. TYPE OF REPORT & PERIOD COVERED:
	6. PERFORMING ORG. REPORT NUMBER:
7. AUTHOR(s): Wolfgang K. Fischer	8. CONTRACT OR GRANT NUMBER(s):
9. PERFORMING ORGANIZATION NAME AND ADDRESS: Naval Underwater Systems Center, New London Laboratory, New London, CT 06320	10. PROGRAM ELEMENT, PROJECT, TASK AREA & WORK UNIT NUMBERS: A12216
11. CONTROLLING OFFICE NAME AND ADDRESS: Naval Sea Systems Command, Washington, DC 20362	12. REPORT DATE: 29 May 1984
	13. NUMBER OF PAGES: 42
14. MONITORING AGENCY NAME & ADDRESS (if different from Controlling Office):	15. SECURITY CLASS. (of this report): UNCLASSIFIED
	15a. DECLASSIFICATION/DOWNGRADING SCHEDULE:

16. DISTRIBUTION STATEMENT (of this Report)

Approved for public release; distribution unlimited.

17. DISTRIBUTION STATEMENT (of the abstract entered in Block 20, if different from Report)

18. SUPPLEMENTARY NOTES

19. KEY WORDS (Continue on reverse side if necessary and identify by block number)

Estimation
Interference Rejection
Matched Filtering
Multi-Target Processing
Time-Delay Estimation

20. ABSTRACT (Continue on reverse side if necessary and identify by block number)

This report describes a technique for obtaining unbiased time delay estimates in the presence of interference. The proposed technique utilizes a matched filter concept wherein the anticipated noise-free generalized cross-correlator (GCC) output between two sensors is matched to the actual received noisy output under a least-mean-square error criterion. Separate unbiased estimates of the target power, target time delay, interference power, interference time delay, and noise power are obtained provided the spectral form of

20. Continued:

the target and interference are known.

The performance of this matched parameter estimator (MPE) is evaluated analytically and compared to the conventional estimator and to MPE simulation results as a function of signal-to-noise, interference-to-noise, time delay separation, and signal and interference spectra. In addition, a potential bias error resulting from a mismatched MPE is also evaluated.

TABLE OF CONTENTS

LIST OF ILLUSTRATIONS

LIST OF SYMBOLS

General

t	time
y_1, y_2, τ	delay time
f	frequency
ω	radial frequency, $2\pi f$
overbar, $\overline{(\ )}$	statistical mean of ( )
overhat, $\hat{(\ )}$	estimate of ( )
oversquiggle, $\tilde{(\ )}$	assumed functional of ( )
prime, $(\ )'$	derivative of ( )
star, $(\ )^*$	complex conjugate of ( )
subscript, $(\ )_j$	partial derivative of ( ) with respect to y_j, j=1,2
subscript, $(\ )_{jk}$	partial derivatives of ( ) with respect to y_j, y_k; j, k=1,2
subscript zero $(\ )_0$	function ( ) is to be evaluated at $y_j = D_j$, j=1,2

Generalized Crosscorrelator (GCC) Symbols

$x_1(t)$	total signal input to channel 1 of the GCC
$x_2(t)$	total signal input to channel 2 of the GCC
$n_j(t)$	noise component of $x_j(t)$, j=1,2
$R_{jj}(\tau)$	autocorrelation function of $x_j(t)$, j=1,2
$R_{12}(\tau)$	crosscorrelation function between $x_1(t)$ and $x_2(t)$
$R_{n_jn_j}(\tau)$	autocorrelation function of $n_j(t)$
$G_{jj}(f)$	auto-spectral density of $x_j(t)$
$G_{12}(f)$	cross-spectral density between $x_1(t)$ and $x_2(t)$
$G_{n_jn_j}(f)$	auto-spectral density of $n_j(t)$
$v(\tau)$, $C(\tau)$	noisy GCC output signal
$n(\tau)$	noise component of the GCC output signal
$N(f)$	Fourier transform of $n(\tau)$
$\delta(f)$	Impulse function
τ_o, $\hat{\tau}_o$	true and estimated value of τ where $C(\tau)$ peaks
T	GCC averaging time

Primary Target Symbols

$s(t)$	primary target signal component of $x_1(t)$
D_1	primary target time delay between channels 1 and 2 of the GCC
$R_1(\tau)$	autocorrelation function of $s(t)$

a_1	primary target signal power
$\rho_1(\tau)$	true, normalized autocorrelation function of s(t)
$\tilde{\rho}_1(\tau)$	assumed, normalized autocorrelation function of s(t)
$G_1(f)$	auto-spectral density of s(t)
$\phi_1(f)$	true, normalized auto-spectral density of s(t)
$\tilde{\phi}_1(f)$	assumed, normalized auto-spectral density of s(t)

Secondary (Interfering) Target Symbols

$I(t)$	secondary target signal component of $x_1(t)$
D_2	secondary target time delay between channels 1 and 2 of the GCC
$R_2(\tau)$	autocorrelation function of I(t)
a_2	secondary target signal power
$\rho_2(\tau)$	true, normalizd autocorrelation function of I(t)
$\tilde{\rho}_2(\tau)$	assumed, normalized autocorrelation function of I(t)
$G_2(f)$	auto-spectral density of I(t)
$\phi_2(f)$	true, normalized auto-spectral density of I(t)
$\tilde{\phi}_2(f)$	assumed, normalized auto-spectral density of I(t)
Δ	time delay separation, D_1-D_2

Matched Parameter Estimator (MPE) Symbols

$J(A_1,A_2,y_1,y_2)$	MPE cost function (to be minimized)
$z(y_1, y_2)$	MPE function to be maximized
$\hat{a}_j$, $\hat{D}_j$	MPE estimates of a_j and D_j, j=1,2
T_1	observation delay time over which J is minimized
Q, $P_j(y_j)$	deterministic, precomputable coefficients of Z, j=1,2
$H_j(y_j)$	Random coefficients of Z, j=1,2
$\beta(y_1,y_2)$	Deterministic part of Z
$\gamma(y_1, y_2)$	Random part of Z
β_{jko}	Various derivatives of β evaluated at $y_j = D_j$ for j, k=1,2
γ_{jo}	Various derivatives of γ evaluated at $y_j = D_j$ for j=1,2
$E_j(f)$	Spectral mismatch between auto-spectral densities, j=1,2
b_j	Bias error of $\hat{D}_j$, j=1,2

IMPROVED MULTI-TARGET TIME DELAY ESTIMATION: MATCHED FILTER APPROACH

INTRODUCTION

The conventional approach to estimate the time delay between two sensors is to crosscorrelate two signals and search for the peak of the resultant crosscorrelation function [1,2]. However, in the presence of interference, these time delay estimates are biased.

Two potential solutions exist for removing this bias: (1) an optimum multitarget processor [3], which requires a basic reformulation of the estimator and (2) a matched filter estimator, which provides additional multitarget processing capability either at the full-beam or split-beam level. This report addresses the methodology and the performance predictions of the latter approach [4] applied at the generalized crosscorrelator (GCC) output.

CONVENTIONAL ESTIMATOR

The GCC is shown in the left portion of figure 1. Assuming that the input to the two channels is

$$x_1(t) = s(t) + I(t) + n_1(t),$$

and

$$x_2(t) = s(t+D_1) + I(t+D_2) + n_2(t), \tag{1}$$

where

$s(t)$ = primary target signal,
$I(t)$ = interfering signal,
$n_1(t)$ = channel 1 input noise,
$n_2(t)$ = channel 2 input noise,
D_1 = desired target time delay, and
D_2 = desired interfering time delay.

Assuming that the signal, interference, and noise are joint Gaussian, zero-mean, uncorrelated processes, it is shown in appendix A that the GCC output $C(\tau)$ for large averaging time T may be represented as

$$C(\tau) = R_{12}(\tau) + n(\tau) = \sum_{j=1}^{2} a_j \rho_j(\tau - D_j) + n(\tau), \tag{2}$$

where $R_{12}(\tau)$ is the noise-free crosscorrelation function between the two channels and $n(\tau)$ is the noise component whose transform has zero-mean and covariance

$$\overline{N(f_1)\, N(f_2)} = \frac{1}{T} [G_{11}(f_1)\, G_{22}(f_1)\, \delta(f_2+f_1) + G_{12}^2(f_1)\, \delta(f_2-f_1)], \tag{3}$$

where a_1 and a_2 are the respective target and interference power; ρ_1 and ρ_2 are the respective normalized target and interference autocorrelation functions; G_{11}, G_{22}, and G_{12} are the respective auto- and cross-spectral densities of channels 1 and 2; and $\delta(f)$ is the familiar impulse function.

The conventional estimator simply searches for the global peak of $C(\tau)$. Denoting $\hat{\tau}_0$ and τ_0 as those values of τ wnere $C(\tau)$ and $R_{12}(\tau)$ peak, respectively, it is shown in appendix B that the mean and variance of $\hat{\tau}_0$ is given by

$$\overline{\hat{\tau}}_0 = \tau_0$$

$$\mathrm{var}(\hat{\tau}_0) = \frac{2\pi}{T} \frac{\int_{-\infty}^{\infty} dw\, w^2 \left(G_{11} G_{22} - G_{12}^2 \, e^{i2w\tau_0} \right)}{\left[\int_{-\infty}^{\infty} dw\, w^2 \, G_{12} \, e^{iw\tau_0} \right]^2}, \tag{4}$$

where τ_0 is the solution to

$$\frac{i}{2\pi} \int_{-\infty}^{\infty} dw\, w\, G_{12}\, e^{i2\tau_0 w} = 0, \tag{5}$$

and

$$w = 2\pi f,$$

$$G_{11}(f) = G_1(f) + G_2(f) + G_{n_1 n_1}(f),$$

$$G_{22}(f) = G_1(f) + G_2(f) + G_{n_2 n_2}(f),$$

and

$$G_{12}(f) = G_1(f)\, e^{-i2\pi f D_1} + G_2(f)\, e^{-i2\pi f D_2},$$

where

G_1 = auto-spectral density of the primary target,
G_2 = auto-spectral density of the interference,
G_{n1n1} = auto-spectral density of the channel 1 input noise, and
G_{n2n2} = auto-spectral density of the channel 2 input noise.

When interference is absent ($G_2 = 0$), the estimator is unbiased, eg., $\hat{\tau}_0 = \tau_0 = D_1$ and

$$\text{var}(\hat{D}_1)\Big|_{\text{single target}} = \frac{2\pi}{T} \frac{\int_{-\infty}^{\infty} dw\, w^2\, (G_{11}G_{22} - G_1^2)}{\left[\int_{-\infty}^{\infty} dw\, w^2\, G_1\right]^2} \quad . \tag{6}$$

This represents the Cramer Rao lower bound for estimating the time delay of a single target in uncorrelated noise and will be used later for normalization purposes.

Figure 2 illustrates the typical bias characteristics of the conventional estimator in the presence of interference. The bias error, $\tau_0 Bw$, is expressed as a function of the reciprocal signal bandwidth, Bw, and is a function of the time-delay separation, $(D_1-D_2)Bw$, between the two interfering targets for the case of flat spectra having unequal bandwidths. Notice the large bias error when the separation is small. Conventional bias reduction schemes tend to suppress the effects of the interfering source by beam shading. We, on the other hand, treat the time-delay estimator in the presence of interference as a two-parameter estimation problem and estimate rather than suppress the interference.

MATCHED PARAMETER ESTIMATOR

A technique for removing the bias error is to match the assumed noise-free GCC output, $\tilde{R}_{12}(\tau)$, to the received noisy GCC output, $C(\tau)$, under a least-mean-square (LMS) error criterion. Accordingly, we wish to minimize the cost function

$$J(A_1, A_2, y_1, y_2) = \int_{-T_{1/2}}^{T_{1/2}} d\tau \left[\sum_{j=1}^{2} A_j\, \tilde{\rho}_j(\tau - y_j) - C(\tau)\right]^2 \quad , \tag{7}$$

where T_1 is the selected observation window and $\tilde{\rho}_j$, $j = 1, 2$ are our assumed normalized autocorrelation functions of the interfering sources. The matched parameter estimator (MPE) is considered to be matched when $\tilde{\rho}_j = \rho_j$ and mismatched when $\tilde{\rho}_j \neq \rho_j$, $j = 1, 2$. The values of A_j, y_j, $j = 1, 2$ at the minimum value of J represent our LMS estimates of a_j, D_j, $j = 1, 2$, respectively.

Because A_1 and A_2 may be determined explicitly, the apparent four-dimensional minimization problem suggested above may be reduced to a two-dimensional maximization scheme. It is shown in appendix C that J is minimized by maximizing

$$z(y_1,y_2) = (P_1H_2^2 + P_2H_1^2 - 2QH_1H_2)/F, \tag{8}$$

and that the estimates of a_1 and a_2 are given by

$$\hat{a}_1 = (P_2\, H_1 - QH_2)/F\Big|_{y_j = \hat{D}_j} \quad , \tag{9}$$

and

$$\hat{a}_2 = (P_1 H_2 - Q H_1)/F \Big|_{y_j = \hat{D}_j}, \tag{10}$$

where

$$Q = \int_{-T_{1/2}}^{T_{1/2}} d\tau\, \tilde{\rho}_1(\tau - y_1)\, \tilde{\rho}_2(\tau - y_2), \tag{11}$$

$$H_j = \int_{-T_{1/2}}^{T_{1/2}} d\tau\, \tilde{\rho}_j(\tau - y_j)\, C(\tau), \quad j = 1, 2, \tag{12}$$

$$P_j = \int_{-T_{1/2}}^{T_{1/2}} d\tau\, \tilde{\rho}_j^2(\tau - y_j), \quad j = 1, 2, \tag{13}$$

and

$$F = P_1 P_2 - Q^2 . \tag{14}$$

Data are usually received at only discrete values of τ rather than continuous values. This modification is easily incorporated in the above expressions by replacing the integral over τ in (7), and (11) through (13) by a summation over the discrete values of τ.

Expressions (8) through (14) represent the working equations of the MPE processor. The implicit solution of (8) for the estimates of D_1 and D_2 requires a two-dimensional peak-searching algorithm which may be facilitated by precomputing and storing the functions P_1, P_2, and Q. Futhermore, the process of locating the global peak of z may be accomplished in either a tracking or acquisition mode. Without apriori knowledge about D_1 and D_2, one needs to search the entire (y_1, y_2) space (acquisition mode). However, as a history of $\hat{D}_1$ and $\hat{D}_2$ is established, the search region may be reduced and (8) may be solved in a tracking mode. Once the global peak has been found, expressions (9) and (10) yield estimates of the primary and interfering target powers, respectively. Finally, the residual $J_{min} = J(\hat{a}_1, \hat{a}_2, \hat{D}_1, \hat{D}_2)$ can serve as a goodness-of-fit indicator. In particular, when the estimator is unbiased, the mean value of J_{min} is simply the total noise power in the observation window, i.e.,

$$\overline{J_{min}} = \int_{-T_{1/2}}^{T_{1/2}} d\tau\, \overline{n^2(\tau)} . \tag{15}$$

PERFORMANCE PREDICTION

It is shown in appendix D that the MPE estimates of D_1, D_2, a_1, and a_2 are unbiased provided the GCC averaging time T is large and the MPE is matched, eg., $\tilde{\rho}_j = \rho_j$. This statement applies regardless of whether the data are discrete or continuous and without restriction on the observation window T_1.

When the estimator is mismatched ($\tilde{\rho}_j \neq \rho_j$), the above estimates will be biased. When the mismatch is small and when $T_1 \to \infty$, it is shown (appendix D) that the mean bias errors of D_1 and D_2 are given approximately by

$$\left.\begin{aligned} \overline{b_1}(\Delta) &= \overline{\hat{D}_1} - D_1 \cong \frac{1}{a_1 \lambda_0} \int_{-\infty}^{\infty} df \; \text{Weg} \; S_1 \\ \overline{b_2}(\Delta) &= \overline{\hat{D}_2} - D_2 \cong \frac{1}{a_2 \lambda_0} \int_{-\infty}^{\infty} df \; \text{Weg} \; S_2 \end{aligned}\right\} \tag{16}$$

where

$$\begin{aligned} S_1 &= \tilde{\phi}_2 \, e^{iw\Delta} \left[\Gamma_{120}(iwF_0 - Q_0 Q_{20}) - \Gamma_{220} Q_{10} P_{10}\right]/F_0 \\ &\quad + \tilde{\phi}_1 \left[\Gamma_{120} Q_{20} P_{20} - \Gamma_{220}(iwF_0 - Q_0 Q_{10})\right]/F_0, \\ S_2 &= \tilde{\phi}_2 \, e^{iw\Delta} \left[\Gamma_{120} Q_{10} P_{10} - \Gamma_{110}(iwF_0 - Q_0 Q_{20})\right]/F_0 \\ &\quad + \tilde{\phi}_1 \left[\Gamma_{120}(iwF_0 - Q_0 Q_{10}) - \Gamma_{110} Q_{20} P_{20}\right]/F_0 \end{aligned} \tag{17}$$

$$\text{Weg} = a_1 E_1 + a_2 E_2 \, e^{-iw\Delta}, \tag{18}$$

$$\lambda_0 = \Gamma_{110} \Gamma_{220} - \Gamma_{120}^2 \quad ,$$

$$\Gamma_{110} = K_{10} - P_{10} Q_{10}^2 / F_0 \; ,$$

$$\Gamma_{220} = K_{20} - P_{20} Q_{20}^2 / F_0 \; ,$$

$$\Gamma_{120} = Q_{120} + Q_0 Q_{10} Q_{20} / F_0 \; ,$$

$$K_{j0} = \int_{-\infty}^{\infty} dt\ w^2\ \tilde{\phi}_j^2 \quad , \ j = 1,\ 2,$$

$$F_0 = P_{10}\ P_{20} - Q_0^2 \ ,$$

$$P_{10} = \int_{-\infty}^{\infty} df\ \tilde{\phi}_1^2 \ ,$$

$$P_{20} = \int_{-\infty}^{\infty} df\ \tilde{\phi}_2^2 \ , \tag{19}$$

$$Q_0 = \int_{-\infty}^{\infty} df\ \tilde{\phi}_1\ \tilde{\phi}_2\ e^{-iw\Delta} \ ,$$

$$Q_{10} = -i \int_{-\infty}^{\infty} df\ w\ \tilde{\phi}_1\ \tilde{\phi}_2\ e^{-iw\Delta} = -\ Q_{20} \ ,$$

$$Q_{120} = \int_{-\infty}^{\infty} df\ w^2\ \tilde{\phi}_1\ \tilde{\phi}_2\ e^{-iw\Delta} \ ,$$

$$w = 2\pi f \quad ,$$

and where ϕ_j, ρ_j and $\tilde{\phi}_j$, $\tilde{\rho}_j$ are Fourier transform pairs; $E_j = \phi_j - \tilde{\phi}_j$, $j = 1, 2$ is the spectral mismatch between the interfering targets; and $\Delta = D_1 - D_2$ is the time delay separation between the two targets.

It is instructive to find an upper bound on the bias error (16). Using (17) and (18), one may show in a straightforward manner that $\int_{-\infty}^{\infty} df\ |S_1|^2 = \Gamma_{220}\ \lambda_0$ and $\int_{-\infty}^{\infty} df\ |S_2|^2 = \Gamma_{110}\ \lambda_0$. Then applying the Schwartz inequality to (16) and using the above result, one obtains

$$|\bar{b}_1|^2 \leq \frac{\Gamma_{220}}{\lambda_0} \int_{-\infty}^{\infty} df \left[E_1 + \left(\frac{a_2}{a_1}\right) E_2\right]^2 \ ,$$

$$|\bar{b}_2|^2 \leq \frac{\Gamma_{110}}{\lambda_0} \int_{-\infty}^{\infty} df \left[\left(\frac{a_1}{a_2}\right) E_1 + E_2\right]^2 \ . \tag{20}$$

The variances of the estimates are derived (in appendix D) under the condition that the MPE is matched and that $T_1 = \infty$. The results are

$$\text{var}\,(\hat{D}_1) = \frac{1}{a_1^2\,\lambda_0^2\,T}\int_{-\infty}^{\infty} df\left[G_{11}\,G_{22}|S_1|^2 + \left(G_{12}^{*}\,S_1\,e^{-iwD_1}\right)^2\right], \tag{21}$$

$$\text{var}\,(\hat{D}_2) = \frac{1}{a_2^2\,\lambda_0^2\,T}\int_{-\infty}^{\infty} df\left[G_{11}\,G_{22}|S_2|^2 + \left(G_{12}^{*}\,S_2\,e^{-iwD_1}\right)^2\right], \tag{22}$$

$$\text{var}\,(\hat{a}_1) = \frac{1}{T}\int_{-\infty}^{\infty} df\left[G_{11}\,G_{22}\,|v_1|^2 + \left(G_{12}^{*}\,v_1\,e^{-iwD_1}\right)^2\right], \tag{23}$$

and

$$\text{var}\,(\hat{a}_2) = \frac{1}{T}\int_{-\infty}^{\infty} df\left[G_{11}\,G_{22}\,|v_2|^2 + \left(G_{12}^{*}\,v_2\,e^{-iwD_1}\right)^2\right], \tag{24}$$

where

$$\begin{aligned} v_1 &= (P_{20}\,\tilde{\phi}_1 - Q_0\,\tilde{\phi}_2\,e^{iw\Delta})/F_0\,, \\ v_2 &= (P_{10}\,\tilde{\phi}_2\,e^{iw\Delta} - Q_0\,\tilde{\phi}_1)/F_0\,, \\ G_{11} &= G_1 + G_2 + G_{n_1n_1}, \\ G_{22} &= G_1 + G_2 + G_{n_2n_2}, \end{aligned} \tag{25}$$

and

$$G_{12}^{*} = e^{iwD_1}\,(G_1 + G_2\,e^{-iw\Delta})\,.$$

A worst case condition occurs when $D_1 = D_2$ ($\Delta = 0$) for which only the spectral characteristics can be used to distinguish between the two interfering targets. Generally this results in the largest variance in the estimates. Under this condition, $Q_{10} = Q_{20} = 0$, S_1 and S_2 are purely imaginary and v_1 and v_2 are real. Expressions (21) through (24) reduce to

$$\text{var}\,(\hat{D}_1)\Big|_{\Delta=0} = \frac{1}{a_1^2\,\lambda_0^2\,T}\int_{-\infty}^{\infty} df\,w^2\,(\tilde{\phi}_2\,\Gamma_{120} - \tilde{\phi}_1\,\Gamma_{220})^2\,G_{-}\,, \tag{26}$$

$$\text{var}\,(\hat{D}_2)\Big|_{\Delta=0} = \frac{1}{a_2^2\,\lambda_0^2\,T}\int_{-\infty}^{\infty} df\,w^2\,(\tilde{\phi}_1\,\Gamma_{120} - \tilde{\phi}_2\,\Gamma_{110})^2\,G_{-}\,, \tag{27}$$

$$\text{var}\,(\hat{a}_1)\Big|_{\Delta=0} \approx \frac{1}{T F_0^2} \int_{-\infty}^{\infty} df\, (P_{20}\, \phi_1 - Q_0\, \phi_2)^2\, G_+ \,, \tag{28}$$

and

$$\text{var}\,(\hat{a}_2)\Big|_{\Delta=0} \approx \frac{1}{T F_0^2} \int_{-\infty}^{\infty} df\, (P_{10}\, \phi_2 - Q_0\, \phi_1)^2\, G_+ \,, \tag{29}$$

where

$$G_- = (G_1 + G_2)\,(G_{n_1 n_1} + G_{n_2 n_2}) + G_{n_1 n_1}\, G_{n_2 n_2},$$

and

$$G_+ = 2(G_1 + G_2)^2 + G_- \,.$$

If in addition to $\Delta=0$ the interfering spectra are identical ($\phi_1 = \phi_2$): then F_0 and Q_0 approach zero and the variances (26) through (29) approach infinity. This is simply an indication that the MPE is unable to distinguish between the two interfering targets under this condition.

RESULTS/DISCUSSION

A convenient figure-of-merit for comparing the performance of the conventional and matched estimators is the normalized degradation ratio (NDR), which is defined as the total rms error in the presence of interference divided by the root-mean-square (rms) error of the conventional estimator in the absence of interference. The latter normalizing term is simply the square root of expression (6). Note that NDR $\geq$ 1 and that large values suggest that the accuracy of the primary target time-delay estimates is seriously degraded in the presence of an interfering target.

Comparisons of the NDR for conventional and matched estimators as well as the corresponding simulation results are shown in figures 3 through 6 for the case of flat spectra and various noise powers. In each case the MPE is assumed to be matched and the signal and noise bands extend from 0 to B (Hz/sec) while the interference occupies the full band (figures 3 and 4) and the upper half band (figures 5 and 6). Additionally, the signal-to-interference ratio (SIR) is 1 dB in all cases. In these figures solid curves represent predicted results for the MPE as obtained from (2[illegible]) while the triangles represent corresponding simulation results. Similarly, the dashed curves represent predicted results for the conventional estimator as obtained from (4), (5), and (6) while the circles represent simulation results. As in figure 2, the time-delay separation is expressed in terms of the reciprocal primary signal bandwidth; eg. we plot NDR as a function of $(D_1 - D_2)B$. Note the excellent agreement between the predicted and simulated results.

When the spectra are identical (figures 3 and 4), the standard deviation of the MPE estimates approaches infinity at zero separation because the target and interference are indistinguishable under this condition. As the separation increases, the matched NDR decays rapidly to a fraction of the

conventional NDR. Note the separation regions where the conventional NDR is smaller than the matched NDR. This is a familiar characteristic that often occurs when comparing biased (conventional) with unbiased (MPE) estimators. At a low signal-to-noise ratio (SNR) the performance improvement is not as dramatic because the random error is much larger than the bias error and swamps its effect (figure 4).

Figures 5 and 6 show an even greater performance improvement because the matched estimator is able to resolve the target and interference at small separations when their spectra are unequal. As before, the improvement degrades at low SNR.

All of the performance improvements in figures 3 through 6 are due to the fact that the MPE estimator is unbiased. This situation occurs only when the assumed interfering spectra are equal to the actual interfering spectra. The sensitivity of the MPE bias error due to a spectral mismatch is illustrated in figure 7 for the case where the primary target spectrum is known (0→B), where the actual interfering target spectrum (ϕ_2) extends from B/2 to B Hz/sec, and the assumed interfering target spectrum ($\tilde{\phi}_2$) has the same bandwidth but a ±13 1/3% center frequency mismatch. This figure may be directly compared to figure 2, which shows the bias error of the conventional estimator for the same spectra and SIR.

Examination of figure 7 reveals that the bias error can be quite large, but is smaller when the center frequency of $\tilde{\phi}_2$ is up-shifted rather than down-shifted. Comparison of figures 2 and 7 shows that the MPE peak bias errors are 2 to 3 times smaller than those of the conventional estimator and that they occur at a smaller time-delay separation. These, as well as other unpublished results, tend to suggest that peak MPE bias errors are usually less than conventional bias errors (even for complete spectral mismatch) and that the smallest peak bias errors are obtained when the higher spectral frequency components are well matched.

CONCLUSION

The MPE technique yields unbiased time-delay estimates in the presence of interference provided the functional form of the interfering spectra are known. In comparison to conventional estimators, rms errors can be reduced several orders of magnitude particularly at high SNR and INR. When the assumed interfering spectra are unequal to the true interfering spectra, the MPE estimates are also biased.

In practice, ápriori information about the primary target spectrum must be known for both conventional and MPE estimators. Thus, the decision to use the MPE rests on what ápriori or measured information exists about the secondary interfering target spectrum. Simulation results tend to suggest that peak MPE bias errors are usually less than corresponding conventional bias errors particularly when the higher spectral frequency components are well matched.

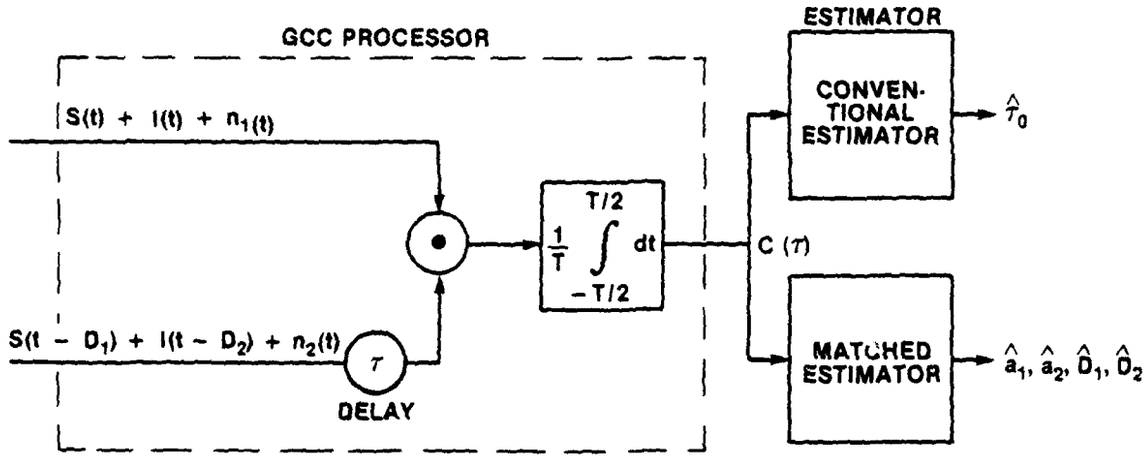

Figure 1. Conventional and Matched Time-Delay Estimators

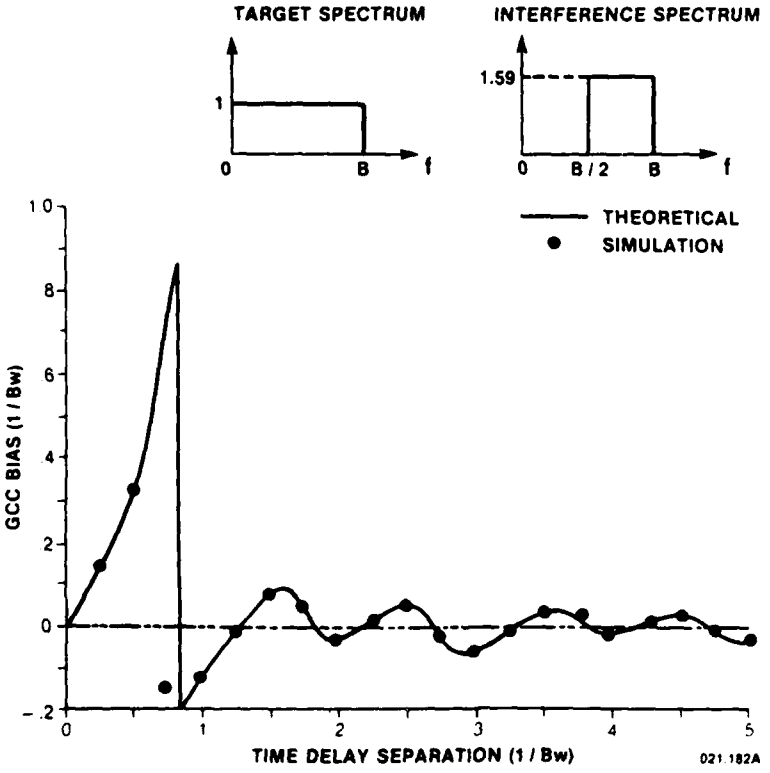

Figure 2. GCC Bias Versus Time-Delay Separation
(SNR = 0 dB, INR = -1 dB; S:0 → B, I:B/2 → B, N:0 → B)

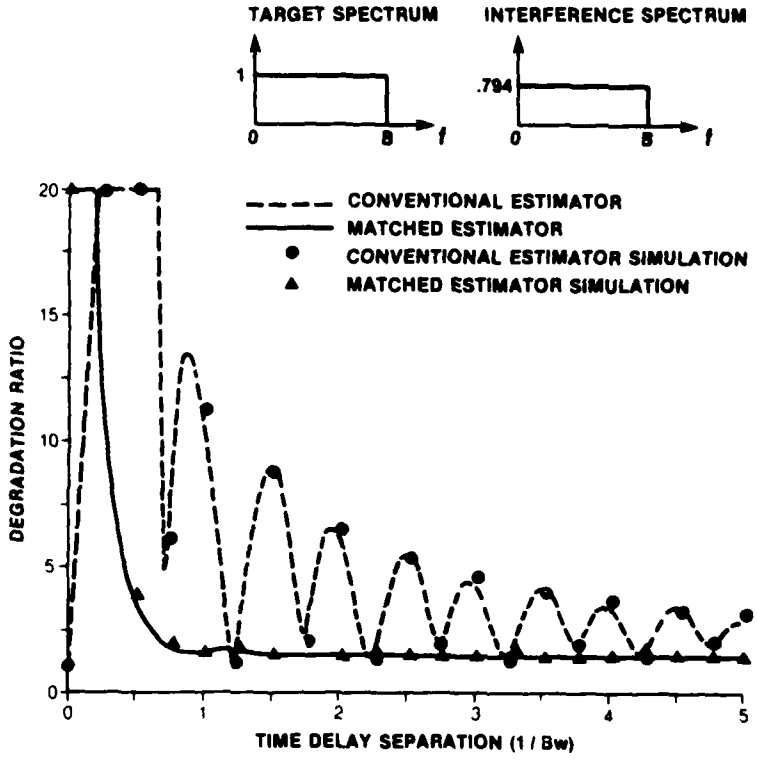

Figure 3. Degration Ratio Versus Time-Delay Separation
(SNR = 0 dB, INR = -1 dB; S:0 → B, I:B/2 → B, N:0 → B)

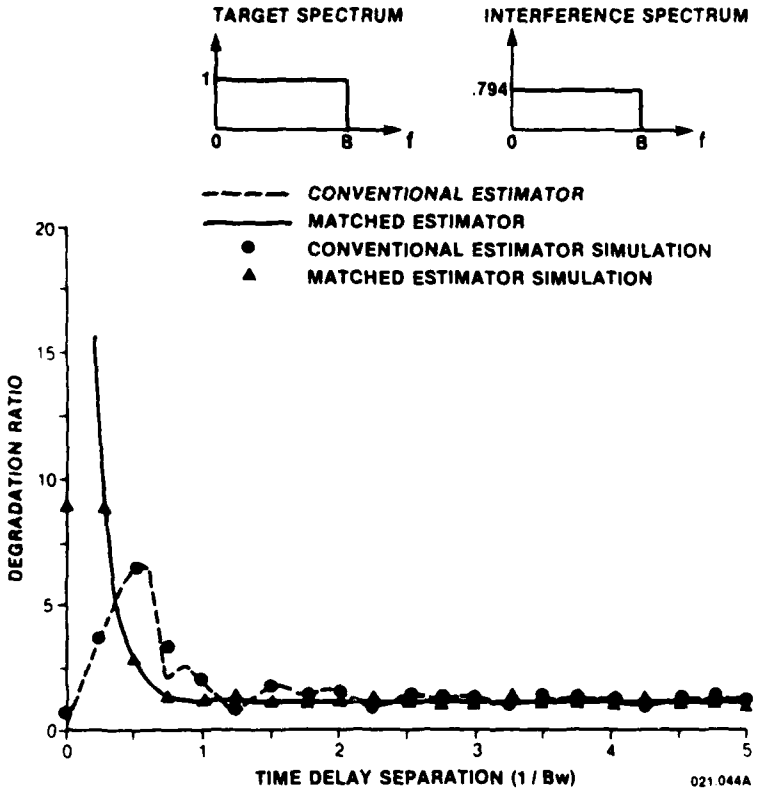

Figure 4. Degration Ratio Versus Time-Delay Separation (SNR = -10 dB, INR = -11 dB; S:0 → B, I:0 → B, N:0 → B)

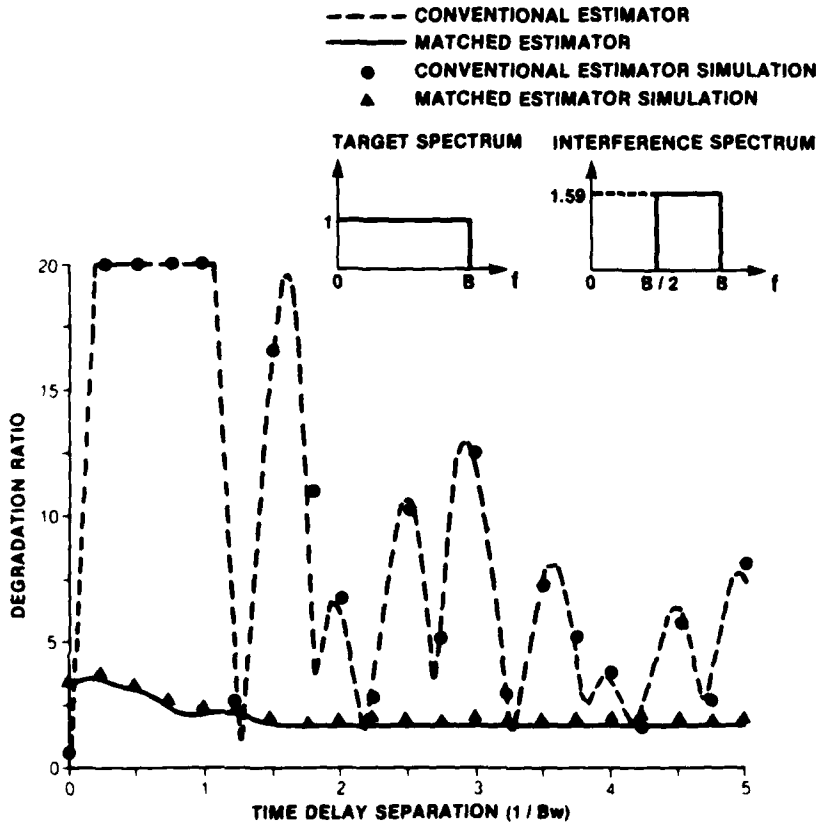

Figure 5. Degration Ratio Versus Time-Delay Separation
(SNR = 0 dB, INR = -1 dB; S:0 → B, I:B/2 → B, N:0 → B)

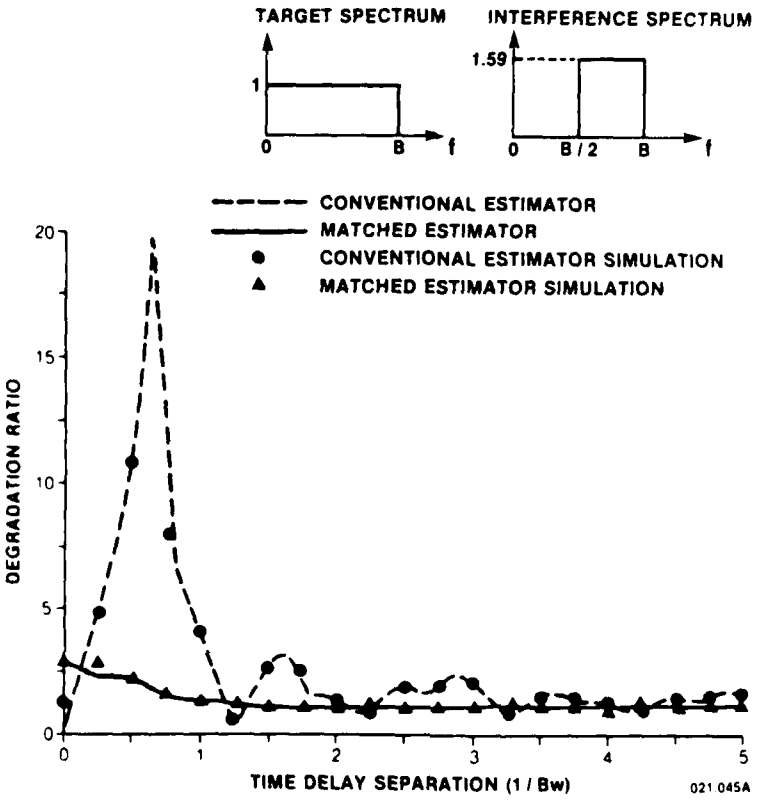

Figure 6. Degration Ratio Versus Time-Delay Separation
(SNR = -10 dB, INR = -11 dB; S:0 → B, I:B/2 → B, N:0 → B)

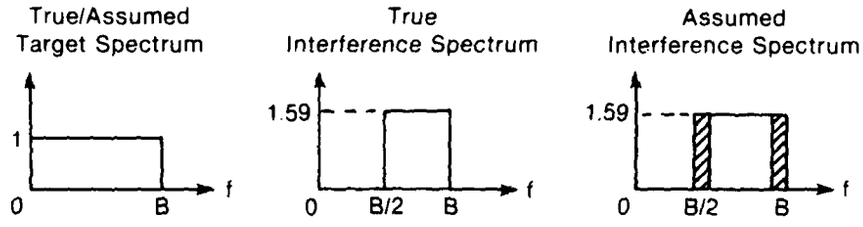

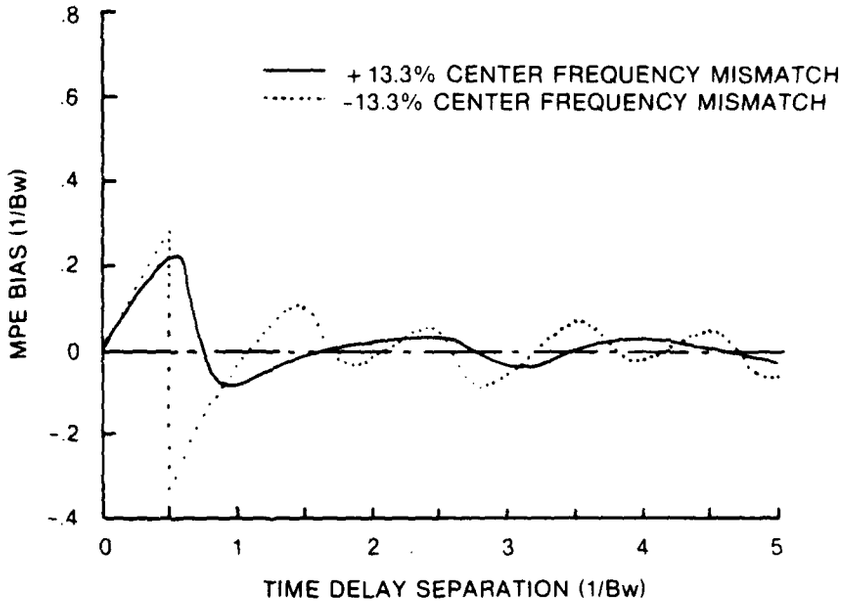

Figure 7. MPE Bias Versus Time-Delay Separation
(SNR = 0 dB, INR = -1 dB; S:0 → B, I:B/2 → B, N:0 → B)

REFERENCES

1. C. H. Knapp and G. C. Carter, "The Generalized Correlation Method for Estimation of Time Delay," IEEE Transaction on Acoustics, Speech and Signal Processing, vol. ASSP-24, August 1976, pp. 320-327.

2. J. C. Hassab and R. E. Boucher, "Optimum Estimation of Time-Delay by a Generalized Correlator," IEEE Transaction on Acoustics, Speech and Signal Processing, vol. ASSP-27, no. 4, August 1979, pp. 373-380.

3. L. C. Ng and Y. Bar-Shalom, "Time Delay Estimation in a Multitarget Environment," Proceedings of the 21st IEEE Conference on Decision and Control, December 1982.

4. W. Fischer and L. Ng, "Improved Time Delay Estimation in the Presence of Interference," IEEE International Conference on Acoustics, Speech and Signal Processing, vol. 2, 1983, p. 899.

APPENDIX A

REPRESENTATION OF THE GENERALIZED CROSSCORRELATOR (GCC) OUTPUT

Referring to the GCC illustrated in figure 1 and the channel inputs (1) described in the text, the GCC output $V(\tau)$ is

$$V(\tau) = \frac{1}{T} \int_{-T/2}^{T/2} dt\; x_1(t)\; x_2(t-\tau) = \frac{1}{T} \int_{-\infty}^{\infty} \Pi\left(\frac{t}{T}\right)\; x_1(t)\; x_2(t-\tau)\; dt, \tag{A-1}$$

where $\Pi\left(\frac{t}{T}\right) = \begin{cases} 1 & |t| \le T/2 \\ 0 & \text{otherwise} \end{cases}$.

Its mean value is

$$\overline{V(\tau)} = \frac{1}{T} \int_{-\infty}^{\infty} dt\; \Pi\left(\frac{t}{T}\right)\; \overline{x_1(t)\; x_2(t-\tau)} = R_{12}(\tau), \tag{A-2}$$

where $R_{12}(\tau)$ is the crosscorrelation function between the two channels.

The covariance of $v(\tau)$ is defined as

$$\mathrm{Cov}(\tau_1, \tau_2) \equiv \overline{v(\tau_1)\; v(\tau_2)} - \overline{v(\tau_1)} \cdot \overline{v(\tau_2)}. \tag{A-3}$$

Substituting (A-1) and (A-2) into (A-3) and using the familiar chain rule for joint Gaussian rv's, one obtains

$$\mathrm{Cov}(\tau_1, \tau_2) = \frac{1}{T^2} \iint_{-\infty}^{\infty} dt_1\; dt_2\; \Pi\left(\frac{t_1}{T}\right)\; \Pi\left(\frac{t_2}{T}\right) [R_{11}(t_1 - t_2)\; R_{22}(t_1 - t_2 + \tau_2 - \tau_1)$$

$$+ R_{12}(t_1 - t_2 + \tau_2)\; R_{12}(\tau_1 + t_2 - t_1)], \tag{A-4}$$

the respective auto and crosscorrelation functions of the two channels, i.e.,

$$R_{11}(\tau) = \overline{x_1(t)\; x_1(t-\tau)} = \sum_{j=1}^{2} a_j\; \rho_j(\tau) + R_{n_1 n_1}(\tau),$$

$$R_{22}(\tau) = \overline{x_2(t)\; x_2(t-\tau)} = \sum_{j=1}^{2} a_j\; \rho_j(\tau) + R_{n_2 n_2}(\tau), \tag{A-5}$$

and

$$R_{12}(\tau) = \overline{x_1(t)\, x_2(t-\tau)} = \sum_{j=1}^{2} a_j\, \rho_j(\tau - D_j),$$

where

$a_j\, \rho_j(\tau) = R_j(\tau)$ = autocorrelation function of the j^{th} target ($j = 1, 2$),
$a_j = R_j(0)$ = power of the j^{th} target ($j = 1, 2$), and
$\rho_j(\tau)$ = normalized autocorrelation function of the j^{th} target ($j = 1, 2$).

Letting $v \equiv t_1 - t_2$ in the integration over t_1 and noting that

$$\int_{-\infty}^{\infty} dt_2\, \Pi\left(\frac{u + t_2}{T}\right) \Pi\left(\frac{t_2}{T}\right) = T\, \Lambda\left(\frac{u}{T}\right), \tag{A-6}$$

where $\Lambda\left(\frac{u}{T}\right) = \begin{cases} 1 - \frac{|u|}{T} & |u| \le T \\ 0 & \text{otherwise} \end{cases}$, (A-4) becomes

$$\mathrm{Cov}(\tau_1, \tau_2) = \frac{1}{T} \int_{-\infty}^{\infty} du\, \Lambda\left(\frac{u}{T}\right) [R_{11}(u)\, R_{22}(u + \tau_2 - \tau_1) + R_{12}(u + \tau_2)\, R_{12}(\tau_1 - u)]; \tag{A-7}$$

and if $T >> |\tau_1| + |\tau_2|$, then

$$\mathrm{Cov}(\tau_1, \tau_2) \approx \frac{1}{T} \int_{-\infty}^{\infty} du\, [R_{11}(u)\, R_{22}(\tau_1 - t_2 - u) + R_{12}(u)\, R_{12}(\tau_1 + t_2 - u)]. \tag{A-8}$$

Now we wish to represent the random GCC output $v(\tau)$ with $C(\tau) = \overline{C(\tau)} + n(\tau)$. In order that these two be equivalent, it follows that $\overline{C(\tau)} = R_{12}(\tau)$, $\overline{n(\tau)} = 0$, and $\overline{n(\tau_1)\, n(\tau_2)} = \mathrm{Cov}(\tau_1, \tau_2)$.

Finally, letting $N(f)$, $n(\tau)$; $G_{11}(f)$, $R_{11}(\tau)$; $G_{22}(f)$, $R_{22}(\tau)$; $G_{12}(f)$, $R_{12}(\tau)$; $G_1(f)$, $R_1(\tau)$; $G_2(f)$, $R_2(\tau)$; $G_{n_1n_1}(f)$, $R_{n_1n_1}(\tau)$; and $G_{n_2n_2}(f)$, $R_{n_2n_2}(\tau)$ be Fourier transform pairs; it follows that $N(f) = 0$ and the covariance

$$\overline{N(f_1)\, N(f_2)} = \iint_{-\infty}^{\infty} d\tau_1\, d\tau_2\, e^{-i2\pi(f_1\tau_1 + f_2\tau_2)}\, \overline{n(\tau_1)\, n(\tau_2)}. \tag{A-9}$$

Substituting (A-8) into (A-9) and performing the indicated integrations, it follows that

$$\overline{N(f_1)\, N(f_2)} = \frac{1}{T} [G_{11}(f_1)\, G_{22}(f_1)\, \delta(f_2 + f_1) + G_{12}^2(f_1)\, \delta(f_2 - f_1)], \tag{A-10}$$

where G_{11}, G_{22}, G_{12} are the respective auto- and cross-spectral densities of the two channels and $\delta(f)$ is the familiar impulse function, i.e.,

$$G_{11}(f) = G_1(f) + G_2(f) + G_{n_1 n_1}(f) ,$$

$$G_{22}(f) = G_1(f) + G_2(f) + G_{n_2 n_2}(f) , \qquad \text{(A-11)}$$

$$G_{12}(f) = G_1(f)\, e^{-i2\pi f D_1} + G_2(f)\, e^{-i2\pi f D_2} ,$$

$$\delta(f) = \begin{cases} \infty & f = 0, \text{ (unit strength)} \\ 0 & \text{otherwise} \end{cases} .$$

APPENDIX B

CONVENTIONAL ESTIMATOR STATISTICS

The conventional time delay estimator locates the global peak of $C(\tau) = R_{12}(\tau) + n(\tau)$ or the zero crossing of its derivative. Denoting τ_0 as the location of the global peak of $R_{12}(\tau)$ and expanding $C'(\tau)$ about τ_0 by means of a Taylor series expansion, one obtains

$$C'(\tau) \cong C'(\tau_0) + (\tau - \tau_0)\, C''(\tau_0) + \ldots, \tag{B-1}$$

where the primes denote differentiations with respect to τ.

Now the estimator finds the value of τ for which $C'(\tau) = 0$. Denoting this value as our estimate $\hat{\tau}_0$, we obtain from (B-1)

$$\hat{\tau}_0 \cong \tau_0 - \frac{C'(\tau_0)}{C''(\tau_0)} \cong \tau_0 - \frac{C'(\tau_0)}{\overline{C''}(\tau_0)}, \tag{B-2}$$

where the latter approximation is valid for high signal-to-noise ratio. Expressing R_{12} and n in terms of their respective Fourier transforms G_{12} and N, we obtain (with $w = 2\pi f$)

$$C'(\tau_0) = n'(\tau_0) = \int_{-\infty}^{\infty} df\ (iw)\ N\, e^{iw\tau_0}, \tag{B-3}$$

and

$$\overline{C''(\tau_0)} = R''(\tau_0) = -\int_{-\infty}^{\infty} df\ w^2\, G_{12}\, e^{iw\tau_0}, \tag{B-4}$$

since $R'(\tau_0) = 0$ (by definition) and $\bar{N} = 0$. It follows that the mean of the estimate $\bar{\tau}_0 = \tau_0$ where τ_0 is the solution to

$$R'(\tau_0) = i \int_{-\infty}^{\infty} df\ w\, G_{12}\, e^{iw\tau_0} = 0. \tag{B-5}$$

Using (B-2) and (B-3), the variance of $\hat{\tau}_0$ is given by

$$\mathrm{var}(\hat{\tau}_0) = \overline{[C'(\tau_0)]^2} \Big/ \overline{[C''(\tau_0)]^2}, \tag{B-6}$$

where

$$\overline{[C'(\tau_0)]^2} = -\iint_{-\infty}^{\infty} df_1\, df_2\, w_1\, w_2\, e^{i\tau_0(w_1 + w_2)}\, \overline{N(f_1)\, N(f_2)}\ . \tag{B-7}$$

Substituting expression (3) of the text into (B-7) and performing the integration with respect to f_2 yields

$$\overline{[C'(\tau_o)]^2} = \frac{1}{T} \int_{-\infty}^{\infty} df\, w^2 \left[G_{11}\, G_{22} - G_{12}^2\, e^{i2w\tau_o}\right] . \qquad (B\text{-}8)$$

Finally, substituting (B-8) and (B-4) into (B-6) and changing the integration variable to w yields expression (4) shown in the text.

APPENDIX C

MINIMIZATION OF THE MATCHED PARAMETER ESTIMATOR (MPE) COST FUNCTION

We wish to minimize the cost function

$$J(A_1, A_2, y_1, y_2) = \int_{-T_{1/2}}^{T_{1/2}} d\tau \, [A_1 \tilde{\rho}_1(\tau - y_1) + A_2 \tilde{\rho}_2(\tau - y_2) - C(\tau)]^2 \qquad (C\text{-}1)$$

by first minimizing J with respect to A_1 and A_2 for the purpose of deriving explicit expressions for A_1 and A_2. Expanding the right side of (C-1), one obtains

$$J = J_0 - 2 A_1 H_1 - 2 A_2 H_2 + A_1^2 P_1 + 2 A_1 A_2 Q + A_2^2 P_2, \qquad (C\text{-}2)$$

where

$$J_0 = \int_{-T_{1/2}}^{T_{1/2}} d\tau \, C^2(\tau) = \text{constant}, \qquad (C\text{-}3)$$

$$H_j(y_j) = \int_{-T_{1/2}}^{T_{1/2}} d\tau \, \tilde{\rho}_j(\tau - y_j) \, C(\tau) \;, \; j = 1, 2, \qquad (C\text{-}4)$$

$$P_j(y_j) = \int_{-T_{1/2}}^{T_{1/2}} d\tau \, \tilde{\rho}_j^{\,2}(\tau - y_j) \qquad , \; j = 1, 2, \qquad (C\text{-}5)$$

and

$$Q(y_1, y_2) = \int_{-T_{1/2}}^{T_{1/2}} d\tau \, \tilde{\rho}_1(\tau - y_1) \, \tilde{\rho}_2(\tau - y_2). \qquad (C\text{-}6)$$

Now differentiating J with respect to A_1, one sees that $\partial J/\partial A_1 = 0$ when A_1 satisfies

$$A_1 = \frac{H_1 - A_2 Q}{P_1} \; . \qquad (C\text{-}7)$$

Substituting (C-7) into (C-2) and collecting terms yields

$$J = J_0 + [A_2^2(P_1 P_2 - Q^2) - 2A_2(H_2 P_1 - H_1 Q) - H_1^2]/P_1. \tag{C-8}$$

Next, differentiating J with respect to A_2, one obtains $\partial J/\partial A_2 = 0$ when A_2 satisfies

$$A_2 = \frac{H_2 P_1 - H_1 Q}{P_1 P_2 - Q^2}. \tag{C-9}$$

Substituting (C-9) into (C-8) and collecting terms results in

$$J = J_0 - z(y_1, y_2), \tag{C-10}$$

where

$$z(y_1, y_2) = \frac{1}{P_1}\left[\frac{(H_2 P_1 - H_1 Q)^2}{(P_1 P_2 - Q^2)} + H_1^2\right] \tag{C-11}$$

$$= \frac{P_1 H_2^2 + P_2 H_1^2 - 2Q H_1 H_2}{(P_1 P_2 - Q^2)} \tag{C-12}$$

Since $Q^2 \leq P_1 P_2$, it follows that $Z > 0$; and since $J_0 > 0$, we deduce that J is a minimum when Z is a maximum. Hence, the apparent four-dimensional minimization of $J(A_1, A_2, y_1, y_2)$ can be achieved by maximizing the two-dimensional function, $z(y_1, y_2)$; and A_2, A_1 can be obtained explicitly from (C-9) and (C-7), respectively.

The function Z has an interesting geometrical interpretation. Dividing both the numerator and denominator of (C-12) by $P_1 P_2$ yields

$$z = (n_1^2 + n_2^2 - 2n_1 n_2 \cos\theta)/\sin^2\theta, \tag{C-13}$$

where

$$n_j = \frac{H_j}{\sqrt{P_j}}, \quad j = 1, 2,$$

and

$$\theta = \cos^{-1}\left(\frac{Q}{\sqrt{P_1 P_2}}\right).$$

In this expression, $n_1^2 = H_1^2/P_1$ is the term that should be maximized if the reference model assumed only the presence of the primary target. This is evident from (C-8) when $A_2 = 0$. Similarly, n_2^2 should be maximized if one assumes only the presence of the interfering source. Considering the triangle formed by the intersection of n_1 and n_2 with acute angle θ; note that, from (C-13), $\sqrt{z} \sin \theta$ is the length of the third side. It follows from plane trigonometry that $\sqrt{z}$ is the diameter of the circle that circumscribes this triangle. Hence, z is directly proportional to the area of the circumscribed circle.

APPENDIX D

STATISTICS OF THE MATCHED PARAMETER ESTIMATOR (MPE) ESTIMATES

In this appendix, we derive the statistics of the MPE estimates $\hat{D}_1$, $\hat{D}_2$, $\hat{a}_1$, and $\hat{a}_2$. In particular, it is demonstrated that, without any restriction on the observation window T_1, the mean estimates are unbiased provided the MPE is matched, eg., $\rho_j = \tilde{\rho}_j$. Expressions for the approximate bias errors of $\hat{D}_1$ and $\hat{D}_2$ are then obtained for large T_1 when the MPE is slightly mismatched. Finally, expressions for the variance of the estimates are derived for both large T_1 and matched conditions.

The bias error associated with estimating the coordinates of the global peak of $z(y_1, y_2)$ may be obtained by expanding the partial derivatives of z about the point (D_1, D_2) via a two-dimensional Taylor series. Using the last subscript 0 to denote that the expression be evaluated at (D_1, D_2) one obtains

$$z_1(y_1, y_2) \cong z_{10} + (y_1 - D_1)\, z_{110} + (y_2 - D_2)\, z_{120}, \tag{D-1}$$

and

$$z_2(y_1, y_2) \cong z_{20} + (y_1 - D_1)\, z_{120} + (y_2 - D_2)\, z_{220}, \tag{D-2}$$

where

$$z_j = \partial z / \partial y_j \quad , \; j = 1, 2,$$

and

$$z_{jk} = \partial^2 z \Big/ \partial y_j \, \partial y_k \quad , \; j, k = 1, 2 \; .$$

Now the search algorithm finds those values of y_1 and y_2 for which the above derivations are zero. Denoting these values as our estimates of D_1 and D_2, respectively, and solving for the resultant bias error, we obtain

$$b_1 = \hat{D}_1 - D_1 = (z_{120}\, z_{20} - z_{220}\, z_{10})/(z_{110}\, z_{220} - z_{120}^2), \tag{D-3}$$

and

$$b_2 = \hat{D}_2 - D_1 = (z_{120}\, z_{10} - z_{110}\, z_{20})/(z_{110}\, z_{220} - z_{120}^2) \; . \tag{D-4}$$

At this point, let us separate the deterministic and random parts of H_j and z by defining

$$h_j(y_j) = \int_{-T_{1/2}}^{T_{1/2}} d\tau \, \rho_j(\tau - y_j)\, R_{12}(\tau), \tag{D-5}$$

and

$$\epsilon_j(y_j) = \int_{-T_{1/2}}^{T_{1/2}} d\tau\, \tilde{\rho}_j(\tau - y_j)\, n(\tau)\ , \tag{D-6}$$

such that $H_j = h_j + \epsilon_j$ for $j = 1, 2$. Substituting these expressions into equation (8) of the text, we obtain

$$z(y_1, y_2) = \beta(y_1, y_2) + \gamma(y_1, y_2), \tag{D-7}$$

where

$$\beta = (P_1 h_2^2 + P_2 h_1^2 - 2 Q h_1 h_2)/F \tag{D-8}$$

$$= h_1 L + h_2 M = (FM^2 + h_1^2)/P_1 = (FL^2 + h_2^2)/P_2, \tag{D-9}$$

$$\gamma = 2(L\epsilon_1 + M\epsilon_2) + (\epsilon_1^2 P_2 + \epsilon_2^2 P_1 - 2Q\, \epsilon_1\, \epsilon_2)/F \tag{D-10}$$

$$\cong 2(L\epsilon_1 + M\epsilon_2) \quad \text{for large } T, \tag{D-11}$$

$$L(y_1, y_2) = (P_2 h_1 - Q h_2)/F = (h_1 - QM)/P_1, \tag{D-12}$$

$$M(y_1, y_2) = (P_1 h_2 - Q h_1)/F = (h_2 - QL)/P_2, \tag{D-13}$$

and

$$F(y_1, y_2) = P_1 P_2 - Q^2\ , \tag{D-14}$$

and where the approximation leading from (D-10) to (D-11) is valid if the GCC averaging time, T, is large. Note that h_j and β are the deterministic parts of H_j and z, respectively; and that $\gamma \to 0$ since $\epsilon_j = 0$.

Now, if both signal-to-noise ratio (SNR) and interference-to-noise ratio (INR) are large, we may replace z_{jk} in (D-3) and (D-4) by β_{jk}; $j, k = 1, 2$. Substituting $z_j = \beta_j + \gamma_j$, $j = 1, 2$, the bias errors reduce to

$$\left.\begin{aligned} b_1 &\cong [\beta_{120}(\beta_{20} + \gamma_{20}) - \beta_{220}\,(\beta_{10} + \gamma_{10})]/(\beta_{110}\,\beta_{220} - \beta_{120}^2) \\ b_2 &\cong [\beta_{120}(\beta_{10} + \gamma_{10}) - \beta_{110}\,(\beta_{20} + \gamma_{20})]/(\beta_{110}\,\beta_{220} - \beta_{120}^2) \end{aligned}\right\} \tag{D-15}$$

where

$$\beta_j = \partial\beta/\partial y_j,$$

$$\gamma_j = \partial\gamma/\partial y_j,$$

and

$$\beta_{jk} = \partial^2\beta/\partial y_j\,\partial y_k \quad , \; j, k = 1, 2 \; .$$

Finally, since $\overline{\gamma} \approx 0$, the mean values of these bias errors are

$$\overline{b_1} \cong (\beta_{120}\,\beta_{20} - \beta_{220}\,\beta_{10})/(\beta_{110}\,\beta_{220} - \beta_{120}^2),$$

and (D-16)

$$\overline{b_2} \cong (\beta_{120}\,\beta_{10} - \beta_{110}\,\beta_{20})/(\beta_{110}\,\beta_{220} - \beta_{120}^2) \; .$$

We must now determine the various derivations of $\beta(y_1, y_2)$ evaluated at $y_1 = D_1$ and $y_2 = D_2$. In order to simplify the notation, we shall use the prime (') to denote differentiation when the expression is a function of only a single variable such as p_j, h_j, and ε_j, and shall continue the subscript notation to denote differentiation when the expression is a function of both y_1 and y_2, such as z, β, γ, Q, L, M, and F.

Using (2), (11), (13), (14), and (D-5) we may show that when $\rho_j = \tilde{\rho}_j$ (matched MPE),

$$\begin{aligned}
&h_{10} = a_1\,P_{10} + a_2\,Q_0 && h_{20} = a_1\,Q_0 + a_2\,P_{20} \\
&h_{10}' = a_1\,P_{10}'/2 + a_2\,Q_{10} && h_{20}' = a_1\,Q_{20} + a_2\,P_{20}'/2 \\
&h_{10}'' = a_1(P_{10}''/2 - K_{10}) + a_2\,Q_{110} && h_{20}'' = a_1\,Q_{220} + a_2(P_{20}''/2 - K_{20}) \\
&F_{10} = P_{10}'\,P_{20} - 2\,Q_0\,Q_{10} && F_{20} = P_{10}\,P_{20}' - 2\,Q_0\,Q_{20} \\
&F_{110} = P_{10}''\,P_{20} - 2\,Q_0\,Q_{110} - 2Q_{10}^2 && F_{220} = P_{10}\,P_{20}'' - 2Q_0\,Q_{220} - 2Q_{20}^2 \\
&\multicolumn{2}{c}{F_{120} = P_{10}'\,P_{20}' - 2Q_0\,Q_{120} - 2Q_{10}\,Q_{20},}
\end{aligned} \qquad \text{(D-17)}$$

where

$$K_j = \int_{-T_{1/2}}^{T_{1/2}} d\tau\,[\tilde{\rho}_j'(\tau - y_j)]^2 \quad , \; j = 1, 2, \qquad \text{(D-18)}$$

and a_1 and a_2 are the signal powers of the primary and interfering targets, respectively.

Using (D-12), (D-13), and (D-17), it may be shown that for the matched MPE

$$\left.\begin{aligned} L_0 &= a_1 & M_0 &= a_2 \\ L_{10} &= \frac{-a_1 F_{10}}{2F_0} & M_{10} &= \frac{a_1}{2F_0}(Q_0 P_{10}' - 2Q_{10} P_{10}) \\ L_{20} &= \frac{a_2}{2F_0}(Q_0 P_{20}' - 2Q_{20} P_{20}) & M_2 &= \frac{-a_2 F_{20}}{2F_0} . \end{aligned}\right\} \quad (D\text{-}19)$$

Now the first order derivatives of β may be obtained from (D-9) and are given by

$$\left.\begin{aligned} \beta_1 &= L(2F_1 + LF_1)/P_2, \\ \beta_1 &= L(2h_1' - 2Q_1 M - LP_1'), \end{aligned}\right\} \quad (D\text{-}20)$$

$$\left.\begin{aligned} \beta_2 &= M(2FM_2 + MF_2)/P_1, \\ \beta_2 &= M(2h_2' - 2Q_2 L - MP_2') \quad . \end{aligned}\right\} \quad (D\text{-}21)$$

Substituting (D-19) into the above expressions at $y_1 = D_1$, $y_2 = D_2$, we obtain that $\beta_{10} = \beta_{20} = 0$. It follows from (D-16) that $\overline{b_1} = \overline{b_2} = 0$, eg., the means of estimates $\hat{D}_1$ and $\hat{D}_2$ are unbiased when the MPE is matched. Also, from equations (9) and (10) of the text, it follows that $\bar{a}_1 = L_0 = a_1$ and $\bar{a}_2 = M_0 = a_2$; hence, the mean power estimates are also unbiased. Notice that no restriction has been imposed on the observation window, T_1, and that the MPE remains unbiased for discrete data, since the integrals are then simply replaced by summations.

The second order derivatives of β are more easily obtained from (D-8). Although tedious, the derivation is straightforward and, when $\rho_j = \tilde{\rho}_j$, yields

$$\beta_{110} = -2a_1^2 \Gamma_{110}, \quad \beta_{220} = -2a_2^2 \Gamma_{220}, \quad \beta_{120} = -2a_1 a_2 \Gamma_{120}, \quad (D\text{-}22)$$

where

$$\left.\begin{aligned} \Gamma_{110} &= K_{10} + \frac{1}{F_0}(P_{10}' Q_0 Q_{10} - P_{10} Q_{10}^2 - P_{20} P_{10}'^2/4), \\ \Gamma_{220} &= K_{20} + \frac{1}{F_0}(P_{20}' Q_0 Q_{20} - P_{20} Q_{20}^2 - P_{10} P_{20}'^2/4), \end{aligned}\right\} \quad (D\text{-}23)$$

and

$$\Gamma_{120} = Q_{120} + \frac{1}{F_0}\left(Q_0\, Q_{10}\, Q_{20} + \frac{P_{10}'\, P_{20}'\, Q_0}{4} - \frac{P_{20}\, P_{10}'\, Q_{20}}{2} - \frac{P_{10}\, P_{20}'\, Q_{10}}{2}\right).$$

When the MPE is mismatched ($\rho_j \neq \rho_j$), all the above estimates will be biased. For a large mismatch, the mean estimates of D_1 and D_2 will be given by the simultaneous solution to $\beta_1 = \beta_2 = 0$. However; when the mismatch is small we may use (D-20) and (D-21) to derive expressions for the approximate bias errors. For this purpose we shall assume $T_1 \to \infty$ and shift our analysis to the frequency domain. Using Parseval's theorem and (D-5), (D-6), (11), and (13), we may express h_j, ε_j, P_j, and Q as

$$h_j = \int df\, \tilde{\phi}_j\, G_{12}^*\, e^{-iwy_j} \qquad , j = 1, 2$$

$$h_j = a_1 \int df\, \tilde{\phi}_j\, \phi_1\, e^{-iw(y_j - D_1)} + a_2 \int df\, \tilde{\phi}_j\, \phi_2\, e^{-iw(y_j - D_2)}, \qquad \text{(D-24)}$$

$$\varepsilon_j = \int df\, \tilde{\phi}_j\, N^*\, e^{-iwy_j} \qquad , j = 1, 2, \qquad \text{(D-25)}$$

$$P_j = \int df\, \tilde{\phi}_j^{\,2} = constant \qquad , j = 1, 2, \qquad \text{(D-26)}$$

and

$$Q = \int df\, \tilde{\phi}_1\, \tilde{\phi}_2\, e^{-iw(y_1 - y_2)}, \qquad \text{(D-27)}$$

where

$$G_{12}(f) = G_1(f)\, e^{-iwD_1} + G_2(f)\, e^{-iwD_2}$$

$$= a_1\, \phi_1\, e^{-iwD_1} + a_2\, \phi_2\, e^{-i2D_2}, \qquad \text{(D-28)}$$

and

$$w = 2\pi f,$$

and where $\tilde{\rho}_j$, $\tilde{\phi}_j$; ρ_j, ϕ_j and n, N are Fourier transform pairs; and all integrations, unless otherwise indicated, are integrated from $-\infty$ to $+\infty$. Defining $E_j = \phi_j - \tilde{\phi}_j$ as the spectral mismatch between the actual and assumed normalized auto-spectral densities, we may then show that at $y_j = D_j$,

$$\left.\begin{aligned} h_{10} &= a_1 P_{10} + a_2 Q_0 + \int df\, \tilde{\phi}_1\, weg \\ h_{10}' &= a_2 Q_{10} - i \int df\, w\, \tilde{\phi}_1\, weg \\ h_{20} &= a_1 Q_0 + a_2 P_{20} + \int df\, \tilde{\phi}_2\, e^{iw\Delta}\, weg \\ h_{20}' &= a_1 Q_{20} - i \int df\, w\tilde{\phi}_2\, e^{iw\Delta}\, weg\ , \end{aligned}\right\} \qquad (D\text{-}29)$$

where

$$weg = a_1 E_1 + a_2 E_2\, e^{-iw\Delta},$$

and

$$\Delta = D_1 - D_2 = \text{time delay separation},$$

and where

$$\left.\begin{aligned} Q_0 &= \int df\, \tilde{\phi}_1\, \tilde{\phi}_2\, e^{-iw\Delta} & P_{10} &= \int df\, \tilde{\phi}_1^2 \\ Q_{10} &= -i \int df\, w\, \tilde{\phi}_1\, \tilde{\phi}_2\, e^{-iw\Delta} = -Q_{20} & P_{20} &= \int df\, \tilde{\phi}_2^2 \\ Q_{120} &= \int df w^2\, \tilde{\phi}_1\, \tilde{\phi}_2\, e^{-iw\Delta} & F_{10} &= -2Q_0\, Q_{10} = -F_{20}. \end{aligned}\right\} \qquad (D\text{-}30)$$

Using (D-12), (D-13), and (D-29), it follows that, for small mismatch,

$$\left.\begin{aligned} L_0 &= a_1 + \int df\, weg\, v_1 \cong a_1 \\ M_0 &= a_2 + \int df\, weg\, v_2 \cong a_2\ , \end{aligned}\right\} \qquad (D\text{-}31)$$

where

$$v_1 = (P_{20}\, \tilde{\phi}_1 - Q_0\, \tilde{\phi}_2\, e^{iw\Delta})/F_0,$$

and

$$v_2 = (P_{10}\, \tilde{\phi}_2\, e^{iw\Delta} - \tilde{Q}_0\, \phi_1)/F_0\ . \qquad (D\text{-}32)$$

Substituting (D-29) and (D-31) into (D-20) and (D-21), one obtains

$$\beta_{10} \cong -2a_1 \int df\ weg(iw\tilde{\phi}_1 + Q_{10}\ v_2),$$

$$\beta_{20} \cong -2a_2 \int df\ weg(iw\tilde{\phi}_2\ e^{iw\Delta} + Q_{20}\ v_1)\ . \tag{D-33}$$

Because the mismatch is assumed to be small, the second order derivatives of β may be replaced by their matched values given in (D-22), where Γ_{jk} in (D-23) reduces to

$$\Gamma_{110} = K_{10} - P_{10}\ Q_{10}^2/F_0,$$

$$\Gamma_{220} = K_{20} - P_{20}\ Q_{20}^2/F_0, \tag{D-34}$$

$$\Gamma_{120} = Q_{120} + Q_0\ Q_{10}\ Q_{20}/F_0\ ,$$

since $T_1 \to \infty$; and $K_j = \int df\ w^2\ \tilde{\phi}_j^2$, $j = 1, 2$.

Finally, substituting (D-22), (D-33), and (D-34) into (D-16), the mean bias errors for a mismatched MPE are given by

$$\bar{b}_1 \cong \frac{1}{a_1\lambda_0} \int df\ weg\ s_1 \quad , \quad \bar{b}_2 \cong \frac{1}{a_2\lambda_0} \int df\ weg\ s_2 \quad , \tag{D-35}$$

where

$$\lambda_0 = \Gamma_{110}\ \Gamma_{220} - \Gamma_{120}^2,$$

$$S_1 = \tilde{\phi}_2\ e^{iw\Delta}\ [\Gamma_{120}(iwF_0 - Q_0\ Q_{20}) - \Gamma_{220}\ Q_{10}\ P_{10}]/F_0$$

$$+ \phi_1[\Gamma_{120}\ Q_{20}\ P_{20} - \Gamma_{220}(iwF_0 - Q_0\ Q_{10})]/F_0, \tag{D-36}$$

$$S_2 = \tilde{\phi}_2\ e^{iw\Delta}\ [\Gamma_{120}\ Q_{10}\ P_{10} - \Gamma_{110}(iwF_0 - Q_0\ Q_{20})]/F_0$$

$$+ \phi_1[\Gamma_{120}(iwF_0 - Q_0\ Q_{10}) - \Gamma_{110}\ Q_{20}\ P_{20}]/F_0\ , \tag{D-37}$$

$$weg = a_1\ E_1 + a_2\ E_2\ e^{iw\Delta}\ .$$

The variance of the estimates shall be derived under matched conditions and for large T_1. Since the estimator is unbiased it follows from (D-15) that

$$\left.\begin{aligned} \mathrm{var}(\hat{D}_1) = \mathrm{var}(b_1) &= \overline{\left(\frac{\beta_{120}\,\gamma_{20} - \beta_{220}\,\gamma_{10}}{\beta_{110}\,\beta_{220} - \beta_{120}^2}\right)^2}\,, \\ \mathrm{var}(\hat{D}_2) = \mathrm{var}(b_2) &= \overline{\left(\frac{\beta_{120}\,\gamma_{10} - \beta_{110}\,\gamma_{20}}{\beta_{110}\,\beta_{220} - \beta_{120}^2}\right)^2}\,, \end{aligned}\right\} \qquad \text{(D-38)}$$

and from (9) and (10), that

$$\left.\begin{aligned} \mathrm{var}(\hat{a}_1) &= \overline{\left(\frac{P_{20}\,\epsilon_{10} - Q_0\,\epsilon_{20}}{F_0}\right)^2}, \\ \mathrm{var}(\hat{a}_2) &= \overline{\left(\frac{P_{10}\,\epsilon_{20} - Q_0\,\epsilon_{10}}{F_0}\right)^2}\,, \end{aligned}\right\} \qquad \text{(D-39)}$$

where, from (D-11) and (D-25),

$$\left.\begin{aligned} \gamma &= 2(L\epsilon_1 + M\epsilon_2), \\ \gamma &= 2\int df\, N^*\,(L\,\tilde{\phi}_1\, e^{-iwy_1} + M\,\tilde{\phi}_2\, e^{-iwy_2})\,. \end{aligned}\right\} \qquad \text{(D-40)}$$

Differentiating the above expression and using (D-19), the derivitives of γ at $y_j = D_j$ become

$$\left.\begin{aligned} \gamma_{10} &= -2a_1 \int df\, N^*\, e^{-iwD_1}\,(iw\tilde{\phi}_1 + Q_{10}\, v_2), \\ \gamma_{20} &= -2a_2 \int df\, N^*\, e^{-iwD_1}\,(iw\tilde{\phi}_2 + Q_{20}\, v_1)\,. \end{aligned}\right\} \qquad \text{(D-41)}$$

Substituting (D-41) and (D-22) into (D-15), the bias errors are given by

$$b_1 = \frac{\int df\ N^*\ e^{-iwD_1}\ S_1}{a_1 \lambda_0}\ ,$$

$$b_2 = \frac{\int df\ N^*\ e^{-iwD_1}\ S_2}{a_2 \lambda_0}\ , \qquad \text{(D-42)}$$

where V_j and S_j have been defined previously. It follows that

$$\text{var}(\hat{D}_1) = \overline{b_1^2}, \qquad \text{(D-43)}$$

$$\text{var}(\hat{D}_1) = \frac{1}{a_1^2\ \lambda_0^2} \iint df_1\ df_2\ \overline{N^*(f_1)\ N^*(f_2)}\ e^{-i2\pi D_1 (f_1 + f_2)}\ S_1(f_1)\ S_1(f_2).$$

Substituting expression (3) of the text into (D-43) and integrating once, we obtain

$$\text{var}(\hat{D}_1) = \frac{1}{a_1^2\ \lambda_0^2\ T} \int df \left[G_{11}\ G_{22}\ |S_1|^2 + \left(G_{12}^*\ S_1\ e^{-iwD_1} \right)^2 \right] . \qquad \text{(D-44)}$$

The variance of $\hat{D}_2$ is obtained in a similar manner from (D-42) and is

$$\text{var}(\hat{D}_2) = \frac{1}{a_2^2\ \lambda_0^2\ T} \int df \left[G_{11}\ G_{22}\ |S_2|^2 + \left(G_{12}^*\ S_2\ e^{-iwD_1} \right)^2 \right] . \qquad \text{(D-45)}$$

Substituting (D-25) into (D-39), one obtains

$$\text{var}(\hat{a}_1) = \overline{\left(\int df\ N^*\ e^{-iwD_1}\ v_1 \right)^2},$$

$$\text{var}(\hat{a}_2) = \overline{\left(\int df\ N^*\ e^{-iwD_1}\ v_2 \right)^2}\ , \qquad \text{(D-46)}$$

where v_1 and v_2 have been defined previously.

From the above discussion, it directly follows that

$$\mathrm{var}(\hat{a}_1) = \frac{1}{T}\int df \left[G_{11}\, G_{22} \left| v_1 \right|^2 + \left(G_{12}^{*}\, e^{-iwD_1}\, v_1 \right)^2 \right]$$

$$\mathrm{var}(\hat{a}_2) = \frac{1}{T}\int df \left[G_{11}\, G_{22} \left| v_2 \right|^2 + \left(G_{12}^{*}\, e^{-iwD_1}\, v_2 \right)^2 \right] . \qquad \text{(D-47)}$$

It should be noted in the above expressions, that weg, $G_{12}^{*}\, e^{-iwD_1}$, S_j, and V_j are functions of Δ so that all the statistics are functions of Δ. Indeed, a detailed inspection of the bias and variance expressions will show that the mean bias errors for the mismatched MPE are odd functions of Δ and the variance expressions are even functions of Δ.

INITIAL DISTRIBUTION LIST

Addressee	No. of of Copies
NAVSEASYSCOM (PMS-409: R. Snugs, M. Roberts, W. Johnson)	2
A&T (H. Jarvis)	1
DTIC	12

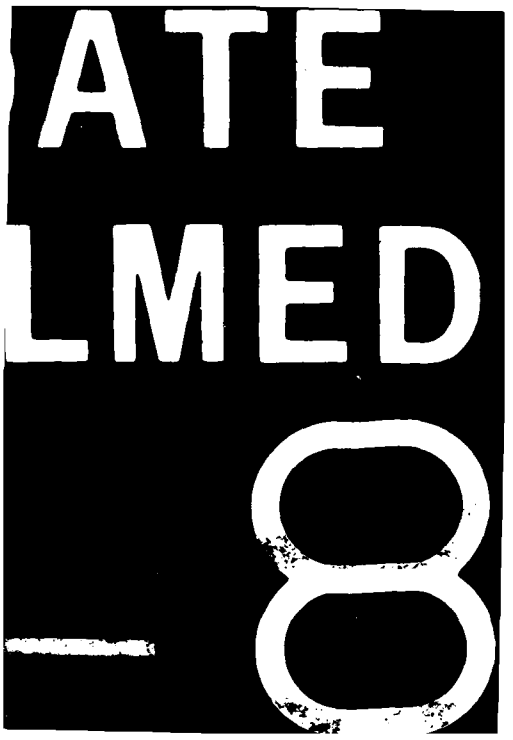
ATE
LMED
8